

Active compliant wall for skin friction reduction



A. Pätzold^{a,*}, I. Peltzer^{a,1}, W. Nitsche^{a,1}, N. Goldin^{b,*}, R. King^{b,1}, D. Haller^{c,*}, P. Woias^{c,1}

^a Technische Universität Berlin, Institute for Aeronautics and Astronautics (ILR), Marchstr. 12-14, 10587 Berlin, Germany

^b Technische Universität Berlin, Chair of Measurement and Control (MRT), Germany

^c University of Freiburg, Department of Microsystems Engineering (IMTEK), Germany

ARTICLE INFO

Article history:

Received 16 October 2012

Received in revised form 27 March 2013

Accepted 29 April 2013

Available online 2 June 2013

Keywords:

Boundary layer

Laminar-turbulent transition

TS-wave control

Active wall

Piezo actuation

Realtime control

ABSTRACT

In order to reduce skin friction drag, an active laminarisation method is developed. Laminar-turbulent boundary layer transition caused by Tollmien–Schlichting (TS) waves is delayed by attenuation of these convective instabilities. An actively driven compliant wall is integrated as part of a wing's surface. Different configurations of piezo-based actuators are combined with an array of sensitive surface flow sensors. Wall-normal actuation as well as inclined wall displacement are investigated. Together with a realtime-control strategy, transition onset is shifted downstream by six average TS-wave lengths. Using the example of flow velocity, the influence of variable flow conditions on TS-damping rates was investigated. Besides, the boundary layer flow downstream of the active wall area as well as required wall deflections and the global damping effect on skin friction are presented in this paper.

© 2013 Elsevier Inc. All rights reserved.

1. Introduction

Laminar-turbulent transition leads to an increase of skin friction by up to one order of magnitude for high Reynolds numbers. Since friction drag accounts for 50% of an aircraft's overall drag, even a small delay of transition onset promises a significant aerodynamic improvement. On two-dimensional and unswept wings, TS-waves are responsible for transition. The natural streamwise amplification of these small velocity fluctuations can be reduced by active damping strategies. The oscillating boundary layer instabilities are coupled to the dampening flow surface. The resulting energy transfer between flow and structure stabilises the boundary layer.

This effect was at first demonstrated by Gaster (1988). Carpenter later designed passive compliant coatings for transition delay and modelled these surfaces by a plate-spring structure (Carpenter and Morris, 1990). One example is depicted in Fig. 1. With a certain damping coefficient, spring constant and inclination angle, a certain wall deflection η arises and maximum transition delay is obtained. The properties of existing materials are not suitable for passive compliant walls in combination with air flows. So the objective of this work is to simulate this compliancy by means of active wave control in wind tunnel experiments. This paper describes the required actuation devices, baseflow investigation, dif-

ferent modes of actuation, application of model predictive control algorithms and the resulting effect on skin friction.

2. Active wall damping and control

Dynamic stabilisation of transitional boundary layers is an effective strategy for drag reduction (Erdmann et al., 2011; Grundmann and Tropea, 2008; Milling, 1981; Opfer et al., 2003; Sturzebecher and Nitsche, 2003). Destructive interference of naturally amplified TS-waves and artificially generated counter waves leads to a significant delay of transition. While manipulating the fluctuation profile of the boundary layer, the mean velocity distribution remains unmodified, see Fig. 2.

The counter waves are generated by discrete actuation strips with intermediate sensors on the wing. Here, the locally restricted actuation is extended towards a large continuous “active compliant wall”. Besides the enlargement of the actuation area, and therefore laminar flow region, sufficient actuation amplitudes decrease.

Fig. 3 illustrates the working principle. Upstream of the active wall, oncoming TS-waves have to be detected for the calculation of appropriate wall deflections. An active wall consists of up to five streamwise actuator elements which are linked by one common surface membrane. By deflection at different nodes within one average TS-wave length, convective travelling counter waves are generated. The actuator-induced velocity fluctuation v_a is then transformed into a streamwise component u_a by the flow itself. Downstream error sensors as well as flow field measurements with movable probes serve for monitoring of the damping performance.

* Corresponding authors.

E-mail address: andreas.paetzold@gmx.de (A. Pätzold).

URL: <http://www.aero.tu-berlin.de> (A. Pätzold).

¹ Principal corresponding author.

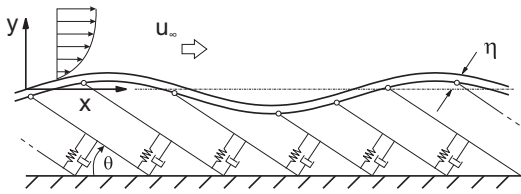


Fig. 1. Model of an anisotropic compliant wall, according to Zengl and Rist (2010).

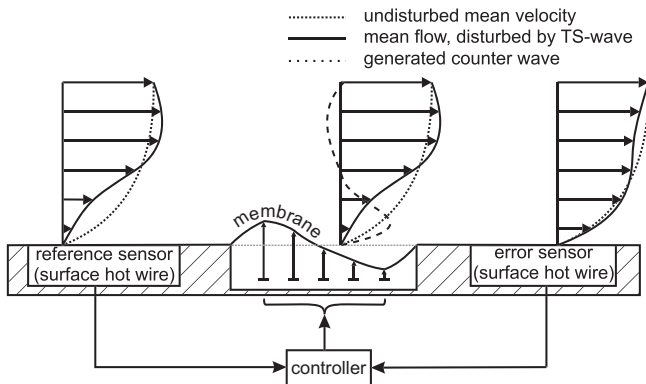


Fig. 2. Destructive interference of TS-wave with artificial travelling wave.

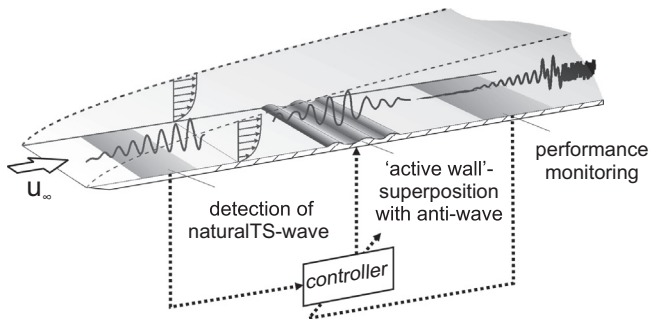


Fig. 3. General principle of an actively controlled wall for TS-wave damping.

Since no intermediate sensors can be installed on top of the membrane, the controller computes several counter wave signals out of one upstream located, global reference sensor. This is done for each actuator element in real time. Therefore, an open-loop model predictive controller (MPC) is implemented (King et al., 2008).

The active wall creates a counter wave which attenuates the TS-wave by negative superposition. In order to estimate the necessary

actuator inputs from upstream flow measurements, models of the involved processes are required. Linear black-box models G_f and G_a simulate the dynamics of the flow and the active wall, respectively. Dotted lines in Fig. 4 symbolise that both transfer functions have to be identified with flow and noise data prior to the damping experiments.

During TS-damping, a control trajectory is determined out of the negative estimated flow signal at error sensor position. In order to induce exactly this trajectory at error sensor position, the MPC-algorithm calculates the required actuator input signals. It solves an optimisation problem for each discrete time step with sampling frequencies around $f_s = 5$ kHz.

3. Experimental setup

The experiments are conducted in a Göttingen-type wind tunnel that is equipped with an unswept two-dimensional wing model in horizontal orientation. It is positioned at half height of the test section and features a modified NACA0008 airfoil with a chord of $c = 1300$ mm. The leading edge is situated 200 mm downstream of the nozzle (see Fig. 5). Because the superposition principle only works within the linear regime of transition, very sensitive surface hot wire sensors are deployed. These surface-mounted hot wires ($\varnothing = 5 \mu\text{m}$) allow for the detection of the very small velocity fluctuations of TS-waves. They generate negligible surface roughness and provide a high signal to noise ratio as well as a 40 kHz cut-off frequency at the used overheat ratio of 1.7. These sensors are not calibrated but adjusted for equal sensitivity. For this purpose a forced turbulent boundary layer is generated.

The maximum freestream turbulence level within the test section is $Tu = 0.3\%$. According to Mack (1984), the corresponding critical N-factor for transition lies between 5 and 5.5. Fig. 12 verifies this relation for the investigated base flow.

Cross talk between high voltage actuator signals and low voltage sensor signals was prevented by noise suppression shielding. Mechanical vibrations were kept from the sensors by a structural decoupling between actuators and sensors as well as an actuator mass damping by a heavy brass suspension plate (see Fig. 10). As a result, no equiphase electronic or mechanical noise can be detected in the sensor signals.

Fig. 6a shows the convective character of transitional instability waves. Besides their typical wave-package shape, no disturbing signal is detected. There is also no thermal vane effect for the chosen streamwise distance between sensors. Fig. 6b illustrates Sig-

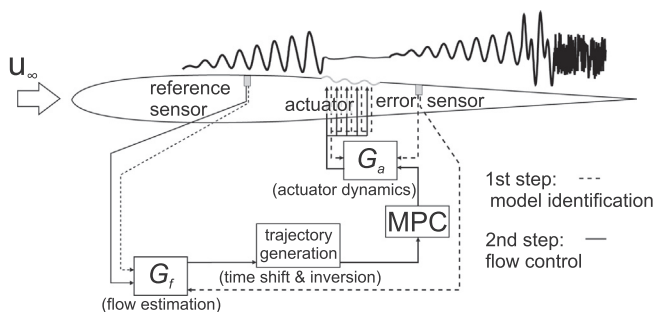


Fig. 4. Model identification and MPC control scheme.

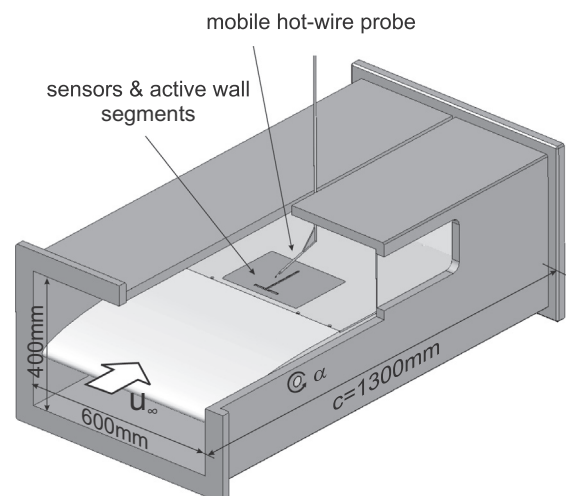


Fig. 5. Test section and wing model with module for sensors and active wall.

Download English Version:

<https://daneshyari.com/en/article/655345>

Download Persian Version:

<https://daneshyari.com/article/655345>

[Daneshyari.com](https://daneshyari.com)